

Theoretical investigation of the inverse Faraday effect via a stimulated Raman scattering process

Daria Popova, Andreas Bringer, and Stefan Blügel

Peter Grünberg Institute and Institute for Advanced Simulation, Forschungszentrum Jülich and JARA, 52425 Jülich, Germany

(Received 15 December 2011; published 14 March 2012)

We study theoretically the origin and mechanism of the ultrafast inverse Faraday effect, which is a magneto-optical effect, attracting much interest nowadays. Laser-induced subpicosecond spin dynamics in hydrogenlike systems and isolated many-electron atoms are investigated in order to get insight into this process. We show that the stimulated Raman scattering process leads to a change of the magnetic state of a system. We obtain the time evolution of the induced magnetization, its dependencies on laser properties, and the connection with the spin-orbit coupling of a system.

DOI: [10.1103/PhysRevB.85.094419](https://doi.org/10.1103/PhysRevB.85.094419)

PACS number(s): 75.78.Jp, 78.20.Ls, 75.60.Jk, 42.65.Dr

INTRODUCTION

Ultrafast optical control of the magnetic state of a medium has recently become a subject of intense research in modern magnetism.^{1,2} The manipulation of a magnetic order by subpicosecond laser pulses is challenging for the development of novel concepts for high-speed magnetic recording, information processing, and data storage. And at the same time, it reveals fundamental questions on magnetization dynamics and makes it possible to understand the fascinating physics of processes, which happen on subpicosecond time scales.

A set of experiments has revealed a direct subpicosecond optical control on magnetization via the inverse Faraday effect, i.e., the process of the generation of a magnetic field by nonlinear polarized light.^{3–5} In these experiments circularly polarized high-intensity laser pulses several tens of femtoseconds long are used to excite a magnetic system of a sample.^{6–14} It was shown that such laser pulses act as an effective magnetic field in oxidic materials, which are weak ferromagnets^{6–10} and even compensated antiferromagnets¹² and paramagnets.¹³ However, the mechanisms of laser-induced magnetization dynamics are still poorly understood in spite of much experimental^{6–18} and theoretical^{19–27} effort.

One of the open questions is the evolution of the magnetic momentum of a medium excited by a laser pulse.^{18,21,24} It cannot be answered without the knowledge of the laser-induced transitions, which lead to the change of the magnetic state of a system in the inverse Faraday effect experiments. In order to get a detailed insight into such transitions, we study the stimulated Raman scattering process, which has been suggested to be responsible for this effect.^{4,9,20} In this process a laser pulse stimulates an optical transition from the ground state to a virtual excited state, which is split due to some interaction, for example, the spin-orbit coupling. Then the transition back to the ground state is stimulated. But due to the transition to the virtual state, the magnetic state of the electron brought back to the ground state is changed. We simulate this process in our systems at the femtosecond time scale and describe the mechanism of how optical transitions, excited by circularly polarized light, can lead to a change of a magnetic state of a system. We investigate the spin dynamics, which accompanied this process, and study how it depends on system and laser properties.

Another question is the role of the spin-orbit coupling (SOC) in the inverse Faraday effect (IFE). It is commonly

accepted that SOC is necessary for magneto-optical effects.⁵ But what is the exact function of this interaction in the process? It is also unclear what happens when the spectral width of the laser pulse is of the order of the SOC and whether it limits the pulse duration required for the effect. We make a detailed study of the laser-induced spin dynamics in a hydrogen atomlike model, in which SOC is present, in order to reveal the pure contribution of this interaction. The simple picture, in which it is the only spin-dependent interaction, allows us to find out its connection with the IFE. We vary the value of the SOC and study how the effect depends on it.

Another important issue, which we address, is the time evolution of the laser-induced magnetization during the presence of the pulse and why the magnetization remains in a system after the excitation, as observed in experiments.^{6–14} We have shown in our last paper²⁸ that the standard expression⁵ $\mathbf{M}(t) \propto \mathbf{E}^*(t) \times \mathbf{E}(t)$, which connects the induced magnetization $\mathbf{M}(t)$ with the generating electric field $\mathbf{E}(t)$, is not applicable for subpicosecond pulses. Therefore, the time dependency of the induced magnetization requires much deeper understanding for the interpretation of the experiments done on a subpicosecond time scale. In the present article, we calculate $\mathbf{M}(t)$ for atomic systems and its dependence on the laser properties. We show that a system is brought to a new magnetic state after the action of an ultrashort laser pulse. The magnetization dynamics after the excitation by a laser is caused by the fact that the system is not in the initial state anymore.^{11,20}

We discuss in the first section the role of optical transitions for the inverse Faraday effect and why much attention should be given for their analysis. We introduce the method, which we use to describe the action of laser light on our systems, in the second section. It is based on the solution of the time-dependent Schrödinger equation. We solve it up to the second order of the inverse light velocity $1/c$ without any further approximations and derive the induced magnetization without the application of thermodynamic relations. We study precisely the time evolution of the involved quantities since it has been pointed out that theories relying on the assumption that the action of the laser light is much shorter than relevant times for the system are not sufficient to describe spin dynamics during the first several picoseconds.¹²

In the next section we introduce the mechanism of the influence of optical transitions on the magnetic state of a system. We study the role of the spin-orbit coupling in this

process and the relation of the effect with its value. We investigate the dependence of the induced magnetization on the laser properties, such as central frequency and intensity, and calculate its time evolution. We use a very simple system in order to make this study very clear and obvious. In the Sec. IV we apply this approach to many-electron atoms as an example of how it can be extended for a more complicated case. We suggest how our theory can be applied for a solid state system in the last section.

I. THE INVERSE FARADAY EFFECT AND THE ULTRAFAST INVERSE FARADAY EFFECT

The inverse Faraday effect was predicted by Pitaevskii³ and was defined by him as “magnetization of a transparent medium induced by oscillating electric field.” It was derived by differentiation of the thermodynamic potential with respect to an external magnetic field. Pershan *et al.*⁴ developed later the theory for this effect based on quantum mechanics. First, they obtained the effective Hamiltonian derived by the time-dependent Schrödinger equation up to the second order. The effective Hamiltonian described the interaction of light with a transparent medium. Since the assumption that the laser intensity “changes slowly compared to thermal relaxation times of the system” was meaningful for the experimental conditions at that time,²⁹ it was possible to derive a potential function from this Hamiltonian. Afterwards it was shown that the induced magnetization is a derivative of this potential. Their formulation of the effect was “the IFE consists of a magnetization induced by circularly polarized light in a nonabsorbing material”. Therefore, the IFE according to Pitaevskii and Pershan *et al.*’s formalisms consists of two processes, which come together: interaction of light with a transparent magnetic medium (IFE-1); this interaction produces a quasistationary relaxed state, which leads to the creation of magnetization in the sample (IFE-2).

The IFE-2 takes place, if the intensity changes slowly compared to thermal relaxation times of the system. In this case the interaction of light with a medium leads to a new thermal equilibrium, because IFE-1 keeps changing the magnetic state of the system and the system has enough time to relax according to the new conditions. This quasistationary state exists only during the presence of the excitation. The IFE-2 process does not take place in the ultrafast magnetization experiments,^{13,28} because the action of the laser pulses is shorter than any relaxation times of a system, and the effects observed in Refs. 6–14 do not represent the IFE according to its classical definition.

However, a kind of the IFE-2 valid for the ultrafast dynamics would be the IFE-2uf process. The IFE-2uf takes place because the system is brought away from its ground magnetic state by transitions induced by circularly polarized laser light. The system has to react to being in this new state; thus magnetic precessions start. There are also some decay processes observed in the next several tenths of a picosecond due to relaxation or damping processes. We suggest that the term “ultrafast IFE” should be meant by the combination of the IFE-1 and IFE-2uf processes.

Magnetization dynamics after the excitation, i.e., the IFE-2uf process, is straightforwardly accessed in the experiments.

Magnetic precessions are the usual target for the problem of all-optical manipulation of a magnetic order.^{1,2,30} However, these effects are initially caused by the action of a laser light on the system, i.e., by the IFE-1 process. Therefore, it is essential to get insight into and characterize the IFE-1 in order to control the subsequent dynamics. The same suggestion was made by Satoh *et al.*¹² and Reid *et al.*,¹³ who both came to the conclusion that the analysis of the evolution of the orbital and spin momenta and the selection rules are necessary for the description of the whole effect.

We consider the IFE-1 process as coherent spin excitations due to the stimulated Raman scattering process. Therefore, we concentrate on the study of the connection between optically induced transitions and the spin state, which we think is the most relevant for the whole ultrafast inverse Faraday effect. We also briefly discuss the IFE-2uf process in Sec. V, where we suggest how our approach can be used to study the spin precessions induced by the optical transitions.

II. THE ACTION OF A LASER FIELD ON AN ELECTRONIC SYSTEM

We consider the action of a laser pulse with a frequency ω_0 and an electric field \mathbf{E} ,

$$\mathbf{E} = -\mathfrak{z}\mathcal{E}f(t/T)\sin(\omega_0 t). \quad (1)$$

on an electronic system with spatial extend much smaller than the wavelength $\lambda_0 = c/\omega_0$. \mathcal{E} is the amplitude of the electric field, \mathfrak{z} is perpendicular to the direction of propagation, and the function $f(t/T)$ describes the time dependence of the amplitude of the electric field.

Let us briefly recall the approach to describe the action of the electric field \mathbf{E} on the system, which was introduced in Ref. 28. The electric field is related to the vector potential³¹

$$\mathbf{E} = -\frac{1}{c}\dot{\mathbf{A}}. \quad (2)$$

The vector potential obeys the wave equation

$$\Delta\mathbf{A} = \left(\frac{\partial}{c\partial t}\right)^2 \mathbf{A} = \frac{1}{c^2}\ddot{\mathbf{A}}, \quad \nabla\mathbf{A} = 0. \quad (3)$$

The spatial extent of the wave train, cT , has to be large compared to the wavelength λ_0 to ensure that \mathbf{A} fulfills Eq. (3).

An unperturbed electronic system is described by the Hamiltonian

$$H_0 = \sum_{\alpha} \mathbf{p}_{\alpha}^2/2 + V_{\text{int}}. \quad (4)$$

\mathbf{p}_{α} is the momentum of an electron, and V_{int} is the sum of the kinetic energy of nuclei, the interaction energy between electrons and nuclei, and the mutual Coulomb energy of the electrons and nuclei. The interactions, which are important for effects on the spin of the electrons, such as the spin-orbit and Zeeman interactions, must be also included in V_{int} . The summation is over all electrons in the system, and the mass and charge of an electron and Planck’s constant are set to 1 (atomic units).

Wave functions of a perturbed electronic system are found by the solution of the time-dependent Schrödinger equation.

The momentum operator is replaced by $\mathbf{p} - \mathbf{A}/c$, and the equation of motion for an electronic wave function Ψ is

$$i \frac{\partial \Psi}{\partial t} = \left[\sum_{\alpha} [\mathbf{p}_{\alpha} - \mathbf{A}(\mathbf{r}_{\alpha}, t)/c]^2/2 + V_{\text{int}} \right] \Psi. \quad (5)$$

The solution is the expansion

$$\Psi(t) = e^{-iH_0 t} [\Psi_0 + \Psi_1(t) + \Psi_2(t) + \dots]. \quad (6)$$

The Raman process, which we are interested in, is of the second order in the inverse speed of light $1/c$. Therefore, the terms up to the third one in the expansion (6) are important. They are derived in Appendix A for the case when the time-dependent function of the amplitude \mathcal{E} of the electric field is Gaussian shaped: $f(t/T) = e^{-t^2/T^2}/\sqrt{\pi}^{3/2}$ (3D normalized).

In the case of a discrete spectrum, the first order wave function is the summation over all possible final states f , which a one photon transition can lead to,

$$\Psi_1(t) = \sum_f d_{0f} \Gamma_f^{(1)}(t) \phi_f, \quad (7)$$

where $d_{0f} = \langle \phi_f | \mathbf{z} \cdot \sum_{\alpha} \mathbf{r}_{\alpha} | \Psi_0 \rangle$ is the dipole matrix element of the transition from the ground state 0 to a final state f , ϕ_f is the wave function of the f state, and the time dependency of $\Psi_1(t)$ is introduced by the function $\Gamma_f^{(1)}(t)$ (cf. Appendix A).

The second order wave function is the summation over all possible intermediate j and final f states, to which the transitions are allowed:

$$\Psi_2(t) = \sum_{j,f} d_{0j} d_{jf} \Gamma_{j,f}^{(2)}(t) \phi_f. \quad (8)$$

The time-dependent function $\Gamma_{j,f}^{(2)}(t)$ is

$$\begin{aligned} \Gamma_{j,f}^{(2)}(t) = & \frac{2(\epsilon_f - \epsilon_j)(\epsilon_j - \epsilon_0)}{\sqrt{\pi}} \left(\frac{NT}{2\pi c} \right)^2 \\ & \times \int_{-\infty}^{t/T} ds' \left[e^{i(\epsilon_f - \epsilon_j)Ts'} \cos(\omega_0 Ts') e^{-s'^2} \right. \\ & \times \left[e^{-\frac{[T(\omega_{0j} + \omega_0)]^2}{4}} \text{erfc} \left(\frac{i}{2} T(\omega_{0j} + \omega_0) - s' \right) \right. \\ & \left. \left. + e^{-\frac{[T(\omega_{0j} - \omega_0)]^2}{4}} \text{erfc} \left(\frac{i}{2} T(\omega_{0j} - \omega_0) - s' \right) \right] \right], \quad (9) \end{aligned}$$

where s' stands for t'/T ; ϵ_0 , ϵ_j , and ϵ_f are the energies of the initial i , an intermediate j , and a final state f ; and $\omega_{kl} = \epsilon_l - \epsilon_k$. k and l stand for 0, j or f .

Equations (8) and (9) are exact for all T , ω_0 , and ω_{0j} , and, therefore, are applicable to any regime of excitation, i.e.,

(a) the ultrafast regime, when the length of the pulse T is in the subpicosecond region ($T|\omega_{0j} \pm \omega_0| \sim 1$) and

(b) the “stationary” regime, when the length of the pulse is in the nanosecond region ($T|\omega_{0j} \pm \omega_0| \gg 1$).

The regime (a) is typically realized in modern magneto-optical experiments,^{1,2} while (b) was the condition of the “classical” inverse Faraday experiment,²⁹ for which the standard theory by Pitaevskii³ and later by Pershan *et al.*⁴ was developed. Equation (8) turns into this theory at large T as follows.²⁸

For large complex arguments $z = |z| e^{i\theta}$, $|z| \rightarrow \infty$, and the polar angle $|\theta| < 3\pi/4$, the function $\text{erfc}(z)$ approaches

asymptotically $\frac{e^{-z^2}}{\sqrt{\pi}z}$.³² From the condition $|\theta| < 3\pi/4$, it follows that $T|\omega_{0j} \pm \omega_0| > 2t/T$, and the condition $T|\omega_{0j} \pm \omega_0| \gg 1$ is necessary for $|z| \rightarrow \infty$. Substituting this asymptote into Eq. (8), one obtains

$$\Psi_2(t) = -i \int_{-\infty}^t \mathcal{H}_{\text{eff}}(t') dt'. \quad (10)$$

The function $\mathcal{H}_{\text{eff}}(t)$ is exactly the effective Hamiltonian, which was defined by Pershan *et al.*⁴ as

$$\langle f | \mathcal{H}_{\text{eff}}(t) | i \rangle = -i \sum_j \left[\frac{v_{0j}(t) v_{jf}^*(t)}{\omega_{0j} + \omega_0} + \frac{v_{jf}(t) v_{0j}^*(t)}{\omega_{0j} - \omega_0} \right] e^{i\omega_{0f} t} \quad (11)$$

with $v_{kl}(t) = d_{kl} E(t)$.

It follows from Eq. (8), that the function $\Gamma_{j,f}^{(2)}(t)$ decreases rapidly, when $T|\omega_{0j} \pm \omega_0|$ becomes larger, but would not feel the change of frequency, when $T|\omega_{0j} \pm \omega_0| \gg 1$. However, the contributions from the levels with energy far away from the resonance frequency to the function $\Gamma_{j,f}^{(2)}(t)$ are negligible in the ultrafast regime ($T|\omega_{0j} \pm \omega_0| \sim 1$).

III. THE HYDROGEN ATOMLIKE SYSTEM EXCITED BY POLARIZED LASER LIGHT

We start from the study of a simple hydrogen atomlike system excited by a laser pulse. We consider the excitation of a Gaussian-shaped laser pulse, which is 100-fs long ($T = 10^{-13}$ s), circularly left polarized, propagating in the z direction, i.e., $\mathbf{z} = (\mathbf{n}_x + i\mathbf{n}_y)/\sqrt{2}$, where \mathbf{n}_x and \mathbf{n}_y are the unit vectors in the x and y directions. We assume that the system is initially in the ground $1s$ state with the spin \mathbf{s}_0 aligned initially in the x direction ($s_{0x} = 1/2$). This means that the wave function of the initial state is $\Psi_0 = Y_{00} R_{1s}(\frac{1}{\sqrt{2}})$, where Y_{00} and R_{1s} are the radial and spherical parts, respectively, of the $1s$ -state wave function. The pulse causes a transition from the ground state to the $2p$ state, which is noticeably split due to the SOC (two orders of magnitude higher than in a real hydrogen atom). The SOC is considered for this system in order to understand the role of this interaction and study the consequence of its variation. Then the transition back to the ground state is stimulated (Fig. 1). We assume that the laser frequency ω_0 is close to the resonance frequency between $1s$ and $2p$ states, and the contribution from the transitions to the other p states can be ignored. The energies ϵ_{1s} and ϵ_{2p} of the $1s$ and $2p$ states are equal to the original ones of a hydrogen

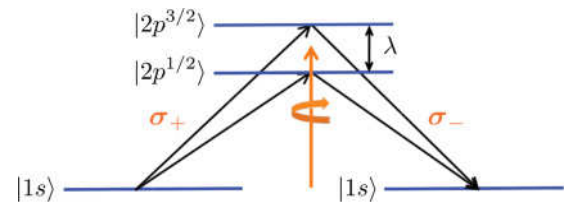


FIG. 1. (Color online) The hydrogen atomlike system excited by a circularly left-polarized pulse. The process designated as σ_+ is the absorption of a left-polarized photon. σ_- is the emission of a left-polarized photon.

atom, and the levels $2p^{1/2}$ and $2p^{3/2}$ are below and above $2p$, respectively: $\epsilon_{2p^{1/2}} = \epsilon_{2p} - (2/3)\lambda$ and $\epsilon_{2p^{3/2}} = \epsilon_{2p} + (1/3)\lambda$, where λ is the value of the SOC. We take $\mathcal{N}T/2\pi d_0\omega_0 c = 1$ for simplicity. We want to answer the two following questions. How would be the orientation of the spin influenced after the two transitions? What is the probability that the spin flip process would take place (the probability to find the spin in the $-x$ direction) due to this process?

These questions can be answered by the second order wave function (8), since it describes two photon transitions, which lead to the Raman process. To obtain this function, we have to calculate the dipole matrix elements of the transitions caused by the laser pulse, and the time-dependent parts $\Gamma_{j,f}^{(2)}(t)$.

A. The second order wave function

The second order wave function $\Psi_2(t)$, which describes the stimulated Raman scattering process, induced by circularly polarized light in our system, is derived in Appendix B:

$$\Psi_2(t) = \frac{|d_0|^2}{\sqrt{2}} \left(\frac{1}{3} \Gamma_{3/2}^{(2)}(t) + \frac{2}{3} \Gamma_{1/2}^{(2)}(t) \right) Y_{00} R_{1s}. \quad (12)$$

The functions $\Gamma_{3/2}^{(2)}(t)$ and $\Gamma_{1/2}^{(2)}(t)$ are the time-dependent parts, which enter Eq. (8), when the intermediate state is $2p^{3/2}$ or $2p^{1/2}$, correspondingly. These functions depend on the energies of initial, intermediate, and final states. Since we assumed that the SOC in our system is considerable and the $2p$ state is split, $\Gamma_{3/2}^{(2)}(t) \neq \Gamma_{1/2}^{(2)}(t)$. For the exact definition of d_0 , see Appendix B.

The second order wave function $\Psi_2(t)$ is a spinor with nonequal time-dependent spin-up and -down parts $[\Gamma_{3/2}^{(2)}(t) \neq \frac{1}{3} \Gamma_{3/2}^{(2)}(t) + \frac{2}{3} \Gamma_{1/2}^{(2)}(t)]$. It means that the spin does not remain in the x direction (the corresponding spinor would be with equal up and down parts), but performs a rotation in time. $\Psi_2(t)$ is zero before the action of the pulse begins, changes smoothly during the excitation, and remains nonzero after the pulse is gone. The time evolution of the function $|\Psi_2(t)|^2$, which is the probability of the Raman scattering process, is depicted on Fig. 2 at laser frequency $\omega_0 = \omega_{1s,2p^{1/2}} - \lambda/2 = \omega_{1s,2p^{3/2}} + \lambda/2$, i.e., between the resonance frequency $\omega_{1s,2p^{1/2}} = (\epsilon_{2p^{1/2}} - \epsilon_{1s})$ of the $1s$ state with the $2p^{1/2}$ state, and the resonance frequency $\omega_{1s,2p^{3/2}} = (\epsilon_{2p^{3/2}} - \epsilon_{1s})$ of the $1s$ state with the $2p^{3/2}$ state. Therefore, it follows from Eq. (12) that the Raman scattering process starts with the action of the pulse and, while the system undergoes this process, the alignment of the spin is changing. Since $\Psi_2(t)$ is nonzero after the action of the pulse, in the end the spin is rotated relative to the initial position.

B. The probability of the spin flip

$$\Psi_2^{\text{In}}(t) \propto Y_{00} R_{1s} \begin{pmatrix} \frac{1}{\sqrt{2}} \\ \frac{1}{\sqrt{2}} \end{pmatrix}. \quad (13)$$

The probability of the spin flip, $w_{\text{sf}}(t)$, that the spin is in the reversed position relative to the initial one after the action of light, is the projection of the wave function of an electron on

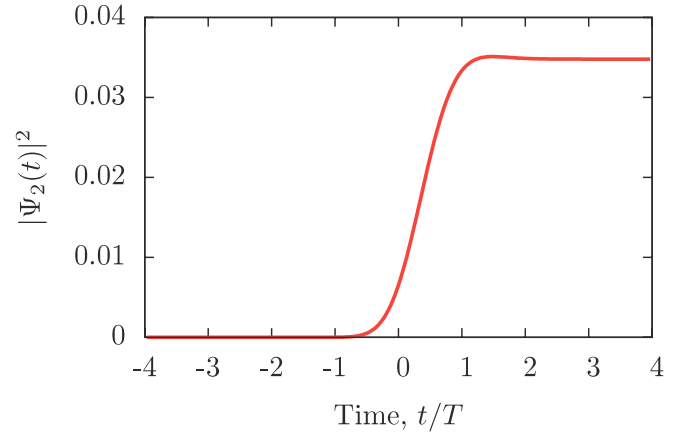


FIG. 2. (Color online) The time evolution of the probability of the Raman scattering process at $\lambda \approx 27$ meV.

the $1s$ state with the spinor $\frac{1}{\sqrt{2}} \begin{pmatrix} 1 \\ -1 \end{pmatrix}$, corresponding to a spin in the $-x$ direction,

$$w_{\text{sf}}(t) = \frac{|\langle \Psi_0 + \Psi_1(t) + \Psi_2(t) | 1s, \frac{1}{\sqrt{2}} \begin{pmatrix} 1 \\ -1 \end{pmatrix} \rangle|^2}{|\Psi_0 + \Psi_1(t) + \Psi_2(t)|^2}. \quad (14)$$

The projections of Ψ_0 and $\Psi_1(t)$ [Eq. (A3)] onto $|1s, \frac{1}{\sqrt{2}} \begin{pmatrix} 1 \\ -1 \end{pmatrix}\rangle$ are zero. The probability of the spin flip is simply

$$w_{\text{sf}}(t) = \frac{|\langle \Psi_2(t) | 1s, \frac{1}{\sqrt{2}} \begin{pmatrix} 1 \\ -1 \end{pmatrix} \rangle|^2}{|\Psi_0 + \Psi_2(t)|^2}. \quad (15)$$

We are interested in the final probability of the spin-flip process in our system. That is, the probability that spin is reversed after the excitation has already acted on a system, causing the two transitions. For this purpose, we define the time τ_p , when the action of the pulse finishes [$E(t > \tau_p) = 0$]. We use $\tau_p = 4T$, when e^{-t^2/T^2} , which describes the amplitude of our pulse, becomes negligible.

Figure 3 shows the probability of the spin-flip process in our system after the action of the laser pulse, $w_{\text{sf}}(\tau_p)$, depending on the excitation frequency at three different values of the SOC. It can be seen that the SOC plays a crucial role in our model. The spin-flip probability is lower at low values of the SOC. But if the SOC is too large, then the probability of the effect is quite low for the excitation frequencies between $\epsilon_{2p^{3/2}}$ and $\epsilon_{2p^{1/2}}$.

It follows from Eq. (12) that if $\lambda = 0$, no rotation of the spin would be observed. Zero or negligible SOC means that $\epsilon_{2p^{3/2}} \approx \epsilon_{2p^{1/2}}$ and, consequently, $\Gamma_{3/2}^{(2)}(t) \approx \Gamma_{1/2}^{(2)}(t)$. Therefore, at any time t the spin-up and -down parts of the spinor (12) would be equal to each other, which is the condition that the spin is in the x direction, and no rotation would be observed. It explains why if λ is too low, the effect starts to disappear. If the SOC is much higher than the spectral width (≈ 20 meV for $T = 100$ fs), the two resonances become isolated.

Another important issue for the effect is the polarization of the laser light. If the light was linear, there would be no spin rotation in the system. It is shown in Appendix C that in the case of the excitation with linear light in any direction, the spinor of the second order wave function would always

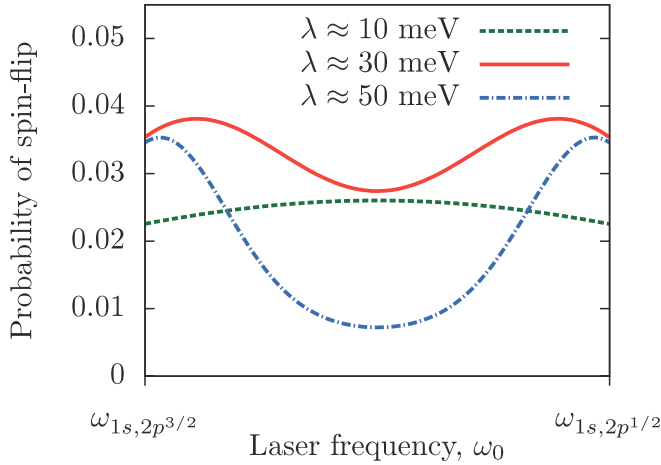


FIG. 3. (Color online) The total probability of the spin flip after the action of the laser pulse depending on the frequency of excitation at different values of λ .

correspond to the alignment of the spin in the x direction and no rotation would be observed.

C. The laser-induced magnetization

We derive the induced magnetization $\Delta \mathbf{M}(t)$ as a function of time for this model. A “direction” (e_x, e_y, e_z) of a spin (which is actually where its mean value maximum points to) with a wave function Ψ' can be determined with the help of the Pauli matrices σ_α (α stands for x, y, z): $e_\alpha = \langle \Psi' | \sigma_\alpha | \Psi' \rangle / |\Psi'|^2$. Taking into account that the electron remains in the initial state with a certain probability, we substitute $\Psi' = \Psi_0 + \Psi_2(t)$ and obtain the new “orientation” of the spin in the s state due to the Raman process. After the subtraction of the initial magnetization and multiplication by the spin magnetic momentum μ , the induced magnetization is obtained:

$$\begin{aligned} \Delta \mathbf{M}(t) &= \mu \left(\frac{\langle \Psi_0 + \Psi_2(t) | \boldsymbol{\sigma} | \Psi_0 + \Psi_2(t) \rangle}{|\Psi_0 + \Psi_2(t)|^2} - \langle \Psi_0 | \boldsymbol{\sigma} | \Psi_0 \rangle \right) \\ &\approx \mu (\langle \Psi_0 | \boldsymbol{\sigma} | \Psi_2(t) \rangle + \langle \Psi_2(t) | \boldsymbol{\sigma} | \Psi_0 \rangle \\ &\quad + \langle \Psi_2(t) | \boldsymbol{\sigma} | \Psi_2(t) \rangle). \end{aligned} \quad (16)$$

Function $\Psi_2(t)$ is proportional to the peak light intensity, $\Psi_2(t) \propto \mathcal{N}^2 \propto \mathcal{E}^2$ [Eqs. (8) and (9)], so are the former two terms. The last term is proportional to the peak intensity squared and can be ignored. Thus, we obtain that the induced magnetization is linear with the light intensity as seen in experiments⁷ due to the interference between the initial and final state, although the probability of such a process is proportional to the intensity squared:

$$\Delta \mathbf{M}(t) \approx \mu (\langle \Psi_0 | \boldsymbol{\sigma} | \Psi_2(t) \rangle + \langle \Psi_2(t) | \boldsymbol{\sigma} | \Psi_0 \rangle). \quad (17)$$

The quantity which the magnetization depends on is the second order wave function $\Psi_2(t)$. This function develops during the action of the pulse and remains constant after the action. Therefore, magnetization in the system is induced via the optical transitions due to the excitation and remains altered after it. As an example the time dependence of the altered components of the magnetization vector due to the excitation with the frequency $\omega_0 = 10.20$ eV at $\lambda = 27.2$ eV is shown on the Fig. 4.

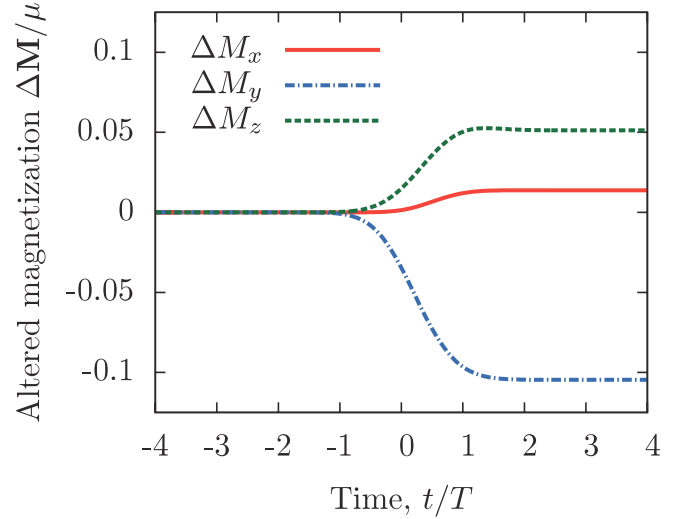


FIG. 4. (Color online) The time dependence of the components of the induced magnetization $\Delta M_{x,y,z}$ at the laser excitation with the frequency $\omega_0 = 10.2$ eV at $\lambda = 27.2$ eV.

In contrast to the equation $\Delta \mathbf{M}(t) \propto \mathbf{E}^*(t) \times \mathbf{E}(t)$, which is usually used to describe the IFE, despite however not providing the answer as to why the change of magnetization is nonzero after the laser pulse has faded away [$\mathbf{E}(\tau_p) = 0 \Rightarrow \Delta \mathbf{M}(\tau_p) \neq 0$], Eq. (16) explains the generation of an effective magnetic field after the excitation by ultrashort laser pulses. According to this relation the magnetization also depends on the electric field $\mathbf{E}(t)$ via $\Psi_2(t)$, but this dependence is much more complicated. In fact, the equation $\Delta \mathbf{M}(t) \propto \mathbf{E}^*(t) \times \mathbf{E}(t)$ is the limit for the case of excitation by very long pulses, when thermodynamic relations can be applied, which was the condition at the time, when it was derived.^{3,4,28,29}

D. The influence of the Raman scattering process on the spin orientation

We study the final spin orientation after the Raman scattering process depending on the excitation frequency. We substitute $\Psi' = \Psi_0 + \Psi_2(\tau_p)$ to $e_\alpha = \langle \Psi' | \sigma_\alpha | \Psi' \rangle / |\Psi'|^2$ and obtain the expectation value of the spin orientation after the excitation has finished.

We vary the laser frequency ω_0 between $\omega_{1s,2p^{3/2}} - 3\lambda$ and $\omega_{1s,2p^{1/2}} + 3\lambda$, covering the region, when the frequency is close to the resonances [“blue” region “b” on Fig. 5(a)] and far away from them [“green” regions “c” on Fig. 5(a)]. We obtain that the frequency dependence of the final spin orientation can be separated into two regimes:

(1) The excitation frequency is close to the resonance. This case is shown on Fig. 5(b). Each blue arrow corresponds to the final spin orientation at a different laser frequency ω_0 , which is varied within the blue region b on Fig. 5(a). When ω_0 is at the “left” boundary of the region b, the spin orientation is close to the initial one. It moves counterclockwise on the plot with the increase of the frequency and arrives again to the position close to the initial one, when the frequency approaches the “right” boundary. At this regime, first, the effect is quite strong (ΔM is large). Second, the direction of the spin is highly affected

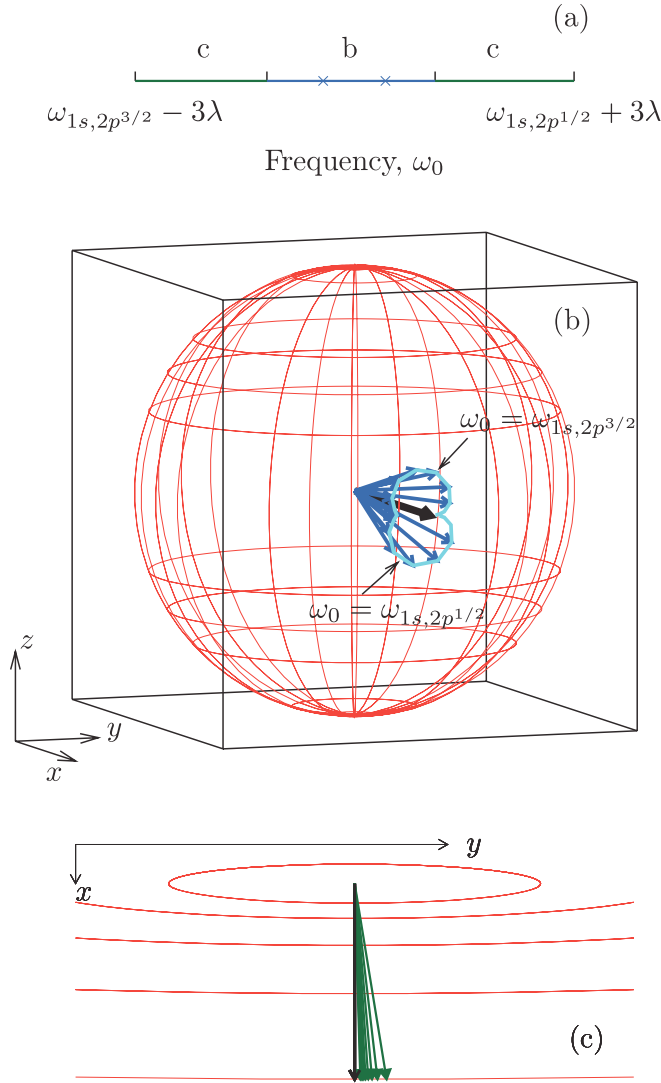


FIG. 5. (Color online) (a) The scale within which the laser frequency is varied. Blue region b corresponds to the plot (b), and green regions c correspond to the plot (c). The blue stars show the exact positions of the resonances (left: $\omega_0 = \omega_{1s,2p^{3/2}}$, right: $\omega_0 = \omega_{1s,2p^{1/2}}$). (b) The final direction of the spin due to the Raman process depending on the frequency of excitation in the resonant region b. It moves counterclockwise on the plot, when ω_0 increases. (c) The final position of the spin due to the Raman process depending on the frequency of excitation in nonresonant regions c, xy plane, the plot is stretched in the y direction. The initial position of the spin is shown with the bold black arrow. $\lambda = 27.2$ meV.

by the excitation frequency. Third, the spin alignment is not in the xy plane.

(2) The situation is quite different, when the frequency is away from the resonances. When the frequency is varied within the regions c on Fig. 5(a), the final spin orientation is always in the xy plane, which is depicted on Fig. 5(c). The effect is much lower in comparison to the resonance regime (1). The final spin direction still depends on the frequency but much less. The plots are similar for the situations, when the frequency decreases in the left region c, and increases in the right region c. When the frequency goes away from the

resonance, the final spin position approaches the initial one from the same “side” in both cases.

The classical interpretation of the IFE^{3,4} is that the circularly polarized laser pulse acts as an external magnetic field in the direction of light propagation z , so it is expected that a spin would start a precession in the xy plane. We have shown that the interpretation of the effect should be different on subpicosecond time scales.²⁸ The change of the initial magnetic state due to laser-induced transitions should be considered, and spin precessions start, because the system is brought away from the ground state. The present example shows that the new spin position after the action of the light is in the xy plane, when the frequency is away from the resonances; however this does not hold for the resonance case. This discrepancy from the classical view may come from the fact that it was developed under the assumption that the excitation is away from any resonance in the system.⁴

The final value of $\Delta M_{x,y,z}$ depends not only linearly on the peak intensity of light, but also on the pulse shape [Eqs. (8) and (9)] and the frequency of excitation (Fig. 5). This statement is supported by the observation in Ref. 14 that the initial phase and amplitude of the oscillation of the polarization of the probe pulse, which is connected with the induced magnetization, depends on the pump wavelength. This result opens large opportunities for tuning spin dynamics by the frequency chirp of a pump laser.

We showed that a laser pulse causes optical transitions, which change the orientation of the spin. Therefore, the laser light can directly transfer the momentum to the spin. The SOC is essential for this process. The existence of this effect is confirmed by the observations of very related processes in quantum wells³³ and quantum dots^{34–36} with an applied external magnetic field in the Voigt geometry.

IV. LASER-INDUCED MAGNETIZATION DYNAMICS IN ISOLATED ATOMS

The next system, in which we investigate the laser-induced ultrafast magnetization phenomenon, is an atomic gas (isolated atoms). A laser pulse causes transitions from the ground state to the excited states of an atom. The excited states are split due to the fine structure. The aim is to look at how this transition influences a magnetic state of an electron brought back to the ground state. We present our results on the cobalt atom, but the same considerations can be applied to any atom.

The essential difference of a many-electron system to a one with a spin $1/2$ is that its spin is composed of several electron spins according to Hund’s rules. Therefore, spin is not a fundamental quantity anymore, and the expectation value of the spin orientation cannot be accessed straightforwardly. The information, which can be obtained, is the probability that the spin is in a certain state and the mean value of the spin $\langle S_\alpha \rangle$ in a chosen direction α . It means that the direction of the maximum mean value of the spin projection cannot be calculated and $\langle S_x \rangle^2 + \langle S_y \rangle^2 + \langle S_z \rangle^2$ is not conserved in the case of a spin larger than $1/2$. The same holds for the total momentum $J > 1/2$.

The ground state of Co is $3d^7 4s^2$ with the total momentum $J = 9/2$, the orbital momentum $L = 3$, and the spin $S = 3/2$. We assume that in the initial state the projection of the

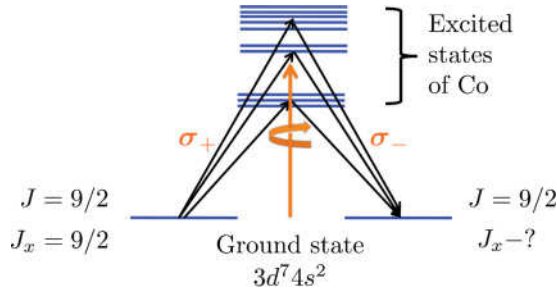


FIG. 6. (Color online) Co atom excited by a circularly left-polarized pulse.

total momentum is defined in the x direction: $J_x = 9/2$. We consider the action of the same laser pulse as in the previous section: 100-fs long, Gaussian shaped, left polarized, propagating in the z direction, being perpendicular to the initial alignment of the magnetic momentum. We account for all excited states to which the laser can cause transitions from the ground state (Fig. 6).

First, we have to find the ground state of the system Ψ_0 by the solution of the equation

$$\hat{j}_x \Psi_0 = (9/2) \Psi_0, \quad (18)$$

where \hat{j}_x is the momentum operator with $(2J+1)(2J+1)$ elements. Since we work in the z representation, the only nonzero elements of the \hat{j}_x matrix are subdiagonal and superdiagonal ones:

$$\begin{aligned} \langle m+1 | \hat{j}_x | m \rangle &= \frac{1}{2} \sqrt{(J-m)(J+m+1)}, \\ \langle m-1 | \hat{j}_x | m \rangle &= \frac{1}{2} \sqrt{(J+m)(J-m+1)}, \\ \langle q | \hat{j}_x | m \rangle &= 0, \quad q \neq m \pm 1. \end{aligned} \quad (19)$$

The resulting ground state wave function in the J_z representation is

$$\Psi_0 = \begin{pmatrix} \psi_{9/2} \\ \psi_{7/2} \\ \vdots \\ \psi_{-9/2} \end{pmatrix} \quad (20)$$

with $2J+1$ elements. It is the superposition of the eigenfunctions of the states with $J_z = m$. For example, $\begin{pmatrix} 0 \\ 1 \\ \vdots \\ 0 \end{pmatrix}$ is the eigenfunction of the state $J_z = 7/2$.

The transitions from the state $\{n, J, J_z = m\}$ via an absorption of a left-polarized photon are allowed to the states $\{n', J' = J, J \pm 1, J'_z = m+1\}$. The reversed process of the stimulated emission leads to the transitions back to $\{n, J, m\}$ with a dipole matrix element, which is the conjugate complex of the dipole matrix element of the first transition.

As $\Psi_2^{n'J'}(t)$ we designate the wave function, which describes the process with two transitions $\{n, J, J_x = 9/2\} \rightarrow$

$\{n', J' = J, J \pm 1, J'_x\} \rightarrow \{n, J, J''_x\}$. Applying Eq. (8), we obtain

$$\Psi_2^{n'J'}(t) = \begin{pmatrix} |\langle n'J' 11/2 | r_+ | nJ 9/2 \rangle|^2 \psi_{9/2} \\ \vdots \\ |\langle n'J' m+1 | r_+ | nJ m \rangle|^2 \psi_m \\ \vdots \\ |\langle n'J' -7/2 | r_+ | nJ -9/2 \rangle|^2 \psi_{-9/2} \end{pmatrix} \Gamma_{n'J'}^{(2)}(t), \quad (21)$$

where $r_+ = (x + iy)/\sqrt{2}$ and $\Gamma_{n'J'}^{(2)}(t)$ is the time-dependent part, which depends also on the energy difference of the states $\{n, J\}$ and $\{n', J'\}$. The dipole matrix elements $\langle J' m + 1 | r_+ | J m \rangle$ can be found using the relations³⁷

$$\begin{aligned} \langle J m + 1 | r_+ | J m \rangle &= \sqrt{\frac{(J-m)(J+m+1)}{J(J+1)(2J+1)}} \langle J | r | J \rangle, \\ \langle J-1 m+1 | r_+ | J m \rangle &= \sqrt{\frac{(J-m)(J-m-1)}{J(2J-1)(2J+1)}} \langle J-1 | r | J \rangle, \\ \langle J+1 m+1 | r_+ | J m \rangle &= -\sqrt{\frac{(J+m+1)(J+m+2)}{(J+1)(2J+1)(2J+3)}} \langle J+1 | r | J \rangle. \end{aligned} \quad (22)$$

We sum up contributions from all possible transitions which lead to the Raman processes and obtain the corresponding second order function

$$\Psi_2^R(t) = \sum_{n'J'} \Psi_2^{n'J'}(t) = \begin{pmatrix} \phi_{9/2} \\ \phi_{7/2} \\ \vdots \\ \phi_{-9/2} \end{pmatrix}. \quad (23)$$

The resulting wave function $\begin{pmatrix} \phi_{9/2} \\ \phi_{7/2} \\ \vdots \\ \phi_{-9/2} \end{pmatrix}$ is not proportional to

the wave function of the ground state, $\begin{pmatrix} \psi_{9/2} \\ \psi_{7/2} \\ \vdots \\ \psi_{-9/2} \end{pmatrix}$, because each

element of the latter spinor was multiplied by a different factor. Consequently, the spinor of the resulting wave function does not correspond to the state with $J_x = 9/2$ anymore, and the projection of the magnetic momentum of the final state is different from the initial one. Therefore, the magnetic state of the system is altered after experiencing the Raman process.

In order to find out how the projection of magnetic momentum has changed, the selection rules should be examined. For the J_x component under an excitation with the vector $(\mathbf{x} + i\mathbf{y})/\sqrt{2}$, they are: for the transition to the intermediate level, the allowed values of the new x projection J'_x are $J_x, J_x \pm 1$; and for ones to the final (ground) state, $J''_x = J_x, J_x \pm 1, J_x \pm 2$. But $J_x = 9/2$ is the maximum value of the projection of $J = 9/2$, and $J''_x = J_x + 1, J_x + 2$ are not possible in our case. Therefore, the possible values of the new

magnetic momentum projection are $J'_x = 9/2, 7/2, 5/2$ after the excitation.

The new projection of magnetic momentum can take each of that values with a certain probability, which depends on the function $\Psi_2(t)$. As $\Psi_{0,J_x=m_x}$ we designate the normalized eigenfunction of the state $\{J = 9/2, J_x = m_x\}$. Then, the probability, that an electron experiences the stimulated Raman scattering process and comes to the ground state with the projection of the magnetic momentum $J_x = m_x$, is the projection of the function $\Psi_2(t)$ on $\Psi_{0,J_x=m_x}$:

$$w_{m_x}(t) = \frac{|\langle \Psi_2^R(t) | \Psi_{0,J_x=m_x} \rangle|^2}{|\Psi_0 + \Psi_1 + \Psi_2|^2}, \quad (24)$$

where $w_{m_x} \neq 0$ for $m_x = 9/2, 7/2, 5/2$. The sum of the functions $w_{m_x}(t)$ is the probability of the Raman-like process, $w_{5/2}(t) + w_{7/2}(t) + w_{9/2}(t) = |\Psi_2^R|^2$. In order to calculate them, we have to know the energies of the excited states $\{n'J'\}$ of Co and the corresponding dipole matrix elements, $\langle n'J' | r | nJ \rangle$. We took this data from the *NIST Atomic Spectra Database*.³⁸

We calculated the probabilities $w_{5/2}(\tau_p)$, $w_{7/2}(\tau_p)$, and $w_{9/2}(\tau_p)$ that the x projection of the magnetic momentum changed to 5/2 or 7/2 or came back to the same state ($J_x = 9/2$) after the laser excitation, accordingly. The results are depicted on Fig. 7 depending on the laser frequency for the excitation by Gaussian-shaped laser pulse with the electric field amplitude $\mathcal{E} = 5 \times 10^7$ V/m, which is a typical value in modern ultrafast magnetization experiments.² For each frequency, the contribution of every allowed excited level is taken into account (see Fig. 6). The three strongest lines on Fig. 7 correspond to the frequencies of the laser in resonance with the most intense transitions in Co (therefore, the probability of the effect becomes higher for these frequencies). Although the case when the projection of the magnetic momentum does not change is most probable, the probability that the value of J_x

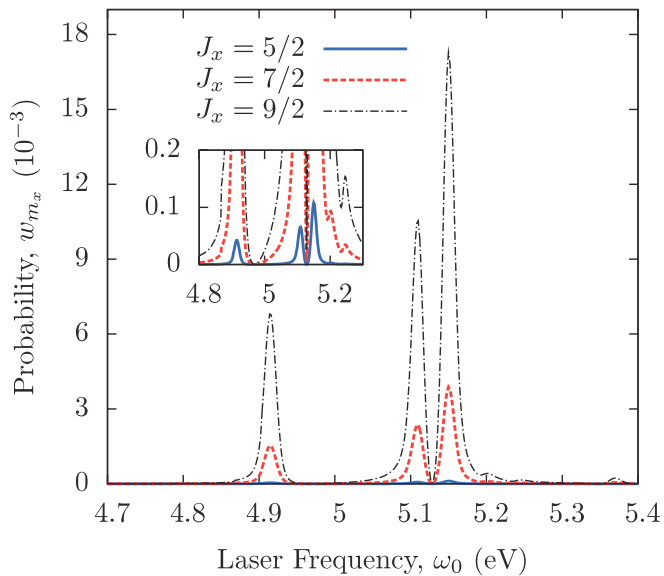


FIG. 7. (Color online) The probabilities of possible values of a new magnetic momentum projection J_x after the Raman scattering process in a Co atom depending on the frequency of excitation. The inset zooms-in on the region where $w_{5/2}$ can be discerned.

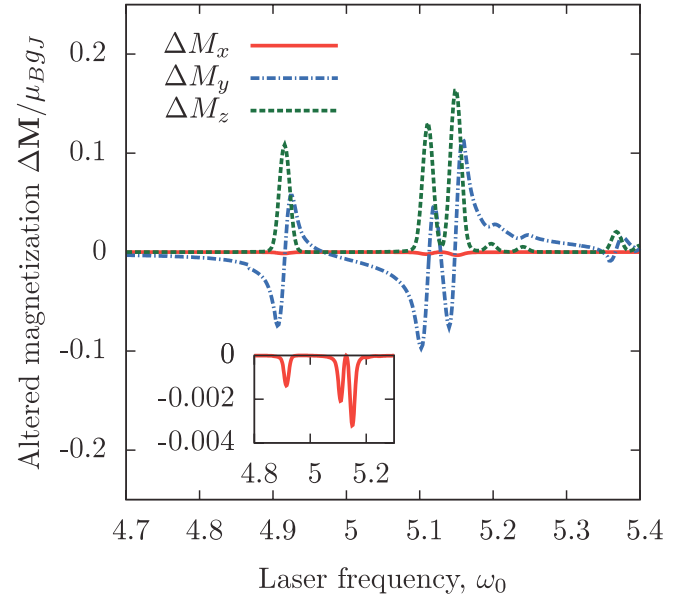


FIG. 8. (Color online) The components of altered magnetization $\Delta \mathbf{M}(\tau_p)$ after the Raman scattering process in a Co atom depending on the frequency of excitation. The inset zooms-in on the region where the ΔM_x component can be discerned.

changes to 7/2 is essential and is nonzero even for the value of 5/2 (see the inset of Fig. 7). It means that the magnetic state of an atom is changed with a certain probability due to transitions caused by laser excitation. Applying analogous considerations as in the previous section, it can be easily shown that the effect is present in isolated atoms, only when the laser light is polarized.

The induced magnetization $\Delta \mathbf{M}(t)$ can be derived by the analogy to the previous section [Eq. (16)].

$$\Delta M_\alpha(t) \approx -\mu_B g_J (\langle \Psi_0 | \hat{J}_\alpha | \Psi_2(t) \rangle + \langle \Psi_2(t) | \hat{J}_\alpha | \Psi_0 \rangle). \quad (25)$$

Here α stays for x, y , and z , \hat{J}_α is the momentum operator, μ_B is Bohr magneton, and g_J is Landé g factor, which for the ground state of Co equals to 5/6. The components of $\Delta \mathbf{M}(\tau_p)$ are depicted on the Fig. 8 at the time $t = \tau_p$, i.e., after the action of the light, depending on the frequency ω_0 of the excitation. The properties of the excitation are the same as for the previous plot. The x component of $\Delta \mathbf{M}(\tau_p)$ is very weak compared to the other components (see the inset of Fig. 8). It results from the selection rules, which do not allow J_x to change more than by 2 and be lower than 5/2 in such a Raman process. This result is in line with the results from Sec. III D.

Strictly speaking, the effect considered in the systems in Secs. III and IV is not the stimulated Raman scattering in the case of zero Zeeman splitting. Stimulated Rayleigh scattering may be a proper term providing the scattering takes place on a particle, which is much smaller compared to the light wave length. However, we always assumed that the spins are initially aligned in a certain direction. This is achieved in experiments by the application of an external magnetic field or taking a magnetically ordered material. Therefore, the magnetic states of a ground state manifold are energetically separated, and the effect is the stimulated Raman scattering.

V. TWO MAGNETIC SUBLATTICES

We briefly discuss in this section the connection between the laser-induced spin excitations, studied above, and the subsequent magnetization dynamics. We consider as an example an antiferromagnetic system with two magnetic vectors \mathbf{M}_{10} and \mathbf{M}_{20} , aligned initially antiparallel to each other, resulting in a total magnetic momentum $\mathbf{M}_0 = \mathbf{M}_{10} + \mathbf{M}_{20}$. A circularly polarized laser pulse coherently acts on this system during several tenths of a femtosecond. Each subsystem is in a new magnetic state after the excitation. The new magnetic vectors are \mathbf{M}_{1l} and \mathbf{M}_{2l} . If the spin systems were initially aligned not in the same directions, then they are rotated by different angles after the action of circularly polarized light (cf. Appendix D). This may simulate two antiferromagnetic sublattices. Therefore, \mathbf{M}_{1l} and \mathbf{M}_{2l} are not collinear anymore. Also, in general $|\mathbf{M}_{1(2)0}| \neq |\mathbf{M}_{1(2)l}|$, as has been shown in Sec. IV.

The two antiferromagnetically coupled subsystems obtain two magnetic vectors now, which are angularly distorted, resulting in the net magnetic moment $\mathbf{M}_l = \mathbf{M}_{1l} + \mathbf{M}_{2l}$. Therefore, the total system is away from the ground state and is in a new magnetic state now. It leads to the IFE-2uf process. The antiferromagnetically coupled magnetic vectors start to precess. The system may also relax from this new state (due to some dissipation effects, damping, and so on) to some stationary state at the next several tenths of a picosecond (the decay observed in experiments).^{1,2}

The final state of a magnetic system can be accessed using the introduced theory. The knowledge of the magnetic state, in which the system is brought due to the excitation, allows one to describe the whole IFE-2uf process.¹¹

CONCLUSIONS

We described the mechanism of the ultrafast inverse Faraday effect via the stimulated Raman scattering process. We solved the time-dependent Schrödinger equation to study the action of the laser light in order to derive correctly the dynamics of the wave functions of involved electrons during the excitation. The simplicity of the investigated systems allowed us to get a detailed insight into the transitions responsible for the change of magnetic states. We showed that a laser pulse excites two electron transitions in the systems: from the initial to the intermediate state and from the intermediate to the ground state, which with a certain probability obtains different magnetic signature then before the excitation. Magnetization due to the action of the pulse is related to this probability. However, it is linearly dependent on the laser peak intensity due to the interference between the initial and final states. The splitting of the intermediate state and the polarization of the laser light were shown to be important for this process. In principle, our formalism is not restricted to the situation when photon is emitted back to the ground state, and can be applied to the situation when initial and final states are different. However, it would make the study more complicated, whereas our goal was to investigate the mechanism on the clearest basis. We hope that this study would encourage further work in understanding the role of the second order transitions for the magneto-optical effects. As

a possibility for future studies, we suggest the investigation of contributions of other interactions which are specific for a solid state and essential for its magnetic state, such as crystal field or Zeeman splitting.

ACKNOWLEDGMENTS

The authors acknowledge the financial support from the FANTOMAS project.

APPENDIX A: THE SOLUTION OF THE TIME-DEPENDENT SCHRÖDINGER EQUATION

We derive the solution of Eq. (5) for the case when the function $f(t/T)$, which describes the time dependence of the amplitude of the electric field \mathbf{E} [see Eq. (1)], is a Gaussian function: $f(t/T) = e^{-t^2/T^2}/\sqrt{\pi}^3$. Expanding the brackets in Eq. (5), we obtain

$$\begin{aligned} i \frac{\partial \Psi}{\partial t} &= \left[\sum_{\alpha} [\mathbf{p}_{\alpha} - \mathbf{A}(\mathbf{r}_{\alpha}, t)/c]^2/2 + V_{\text{int}} \right] \Psi \\ &= \left[H_0 - \frac{1}{c} \sum_{\alpha} \mathbf{A}(\mathbf{r}_{\alpha}, t) \mathbf{p}_{\alpha} + \frac{1}{2c^2} \sum_{\alpha} \mathbf{A}(\mathbf{r}_{\alpha}, t)^2 \right] \Psi \\ &= [H_0 + H_p] \Psi \end{aligned} \quad (\text{A1})$$

The solution is found using the Volterra iteration method and is the expansion

$$\begin{aligned} \Psi(t) &= e^{-iH_0 t} [\Psi_0 + \Psi_1(t) + \Psi_2(t) + \dots] \\ &= e^{-iH_0 t} \left[1 - i \int_{-\infty}^t \bar{H}_p(t') dt' - \int_{-\infty}^t \bar{H}_p(t') dt' \right. \\ &\quad \left. \times \int_{-\infty}^{t'} \bar{H}_p(t'') dt'' + \dots \right] \Psi_0 \end{aligned} \quad (\text{A2})$$

with $\bar{H}_p(t) = e^{iH_0 t} H_p(t) e^{-iH_0 t}$.

The Raman process, which we are interested in, is of the second order in the inverse speed of light $1/c$. Therefore, the terms up to the third one in the expansion (A2) are important.

In the case of a discrete spectrum, the first order wave function is the summation over all possible final states, which a one photon transition can lead to,

$$\Psi_1(t) = \sum_f I_{1,f}(t) \phi_f \quad (\text{A3})$$

with the transition amplitudes $I_{1,f}$,

$$I_{1,f}(t) = -i \int_{-\infty}^t dt' e^{i(\epsilon_f - \epsilon_0)t'} \langle \phi_f | H_p(t') | \Psi_0 \rangle, \quad (\text{A4})$$

where ϵ_f and ϵ_0 are the energies of the final state f and the ground state 0, respectively, and ϕ_f is the wave function of the f state. The transition amplitudes (A4) are

$$\begin{aligned} I_{1,f}(t) &= \frac{i}{c} \langle \phi_f | \sum_{\alpha} \mathbf{p}_{\alpha} | \Psi_0 \rangle \\ &\quad \times \int_{-\infty}^t dt' e^{i(\epsilon_f - \epsilon_0)t'} \cos(\omega_0 t) \mathcal{N} e^{-t^2/T^2}. \end{aligned} \quad (\text{A5})$$

The matrix element of the momentum operator can be conveniently expressed by the dipole operator $\mathcal{D} = \sum_{\alpha} \mathbf{r}_{\alpha}$ using the relation $i \sum_{\alpha} \mathbf{p}_{\alpha} = (\epsilon_f - \epsilon_0) \mathcal{D}$; then

$$I_{1,f}(t) = \frac{(\epsilon_f - \epsilon_0)}{c} \langle \phi_f | \mathcal{D} | \Psi_0 \rangle \times \int_{-\infty}^t dt' e^{i(\epsilon_f - \epsilon_0)t'} \cos(\omega_0 t) \mathcal{N} e^{-t^2/T^2}. \quad (\text{A6})$$

For convenience we introduce the function $\Gamma_f^{(1)}(t)$, which is defined by the relation

$$I_{1,f}(t) = \langle \phi_f | \mathcal{D} | \Psi_0 \rangle \Gamma_f^{(1)}(t). \quad (\text{A7})$$

Using the solution of the Fourier integral³⁹

$$\int_{-\infty}^s ds' e^{i w_{\pm} s'} e^{-s'^2} = \frac{\sqrt{\pi}}{2} e^{-\frac{w_{\pm}^2}{4}} \text{erfc}\left(\frac{i}{2} w_{\pm} - s\right), \quad (\text{A8})$$

and replacing s by t/T and w_{\pm} by $T(\epsilon_f - \epsilon_0 \pm \omega_0)$, we obtain the time dependence of

$$\Gamma_f^{(1)}(t) = \frac{\mathcal{N} T (\epsilon_f - \epsilon_0)}{2\pi c} \times \left[e^{-\frac{[T(\omega_0 f + \omega_0)]^2}{4}} \text{erfc}\left(\frac{i}{2} T(\omega_0 f + \omega_0) - \frac{t}{T}\right) + e^{-\frac{[T(\omega_0 f - \omega_0)]^2}{4}} \text{erfc}\left(\frac{i}{2} T(\omega_0 f - \omega_0) - \frac{t}{T}\right) \right]. \quad (\text{A9})$$

with $\omega_0 f = \epsilon_f - \epsilon_0$ and \mathcal{N} being the normalization factor of the wave train.

Finally, the time evolution of the function $\Psi_1(t)$ is

$$\Psi_1(t) = \sum_f d_{0f} \Gamma_f^{(1)}(t) \phi_f, \quad (\text{A10})$$

where $d_{0f} = \langle \phi_f | \mathcal{D} | \Psi_0 \rangle$ is the dipole matrix element of the transition from the ground state 0 to the final state f .

In the similar way the second order wave function can be found:

$$\begin{aligned} \Psi_2(t) &= -i \int_{-\infty}^t dt' \bar{H}_p(t') \Psi_1(t') \\ &= -i \int_{-\infty}^t dt' \bar{H}_p(t') \sum_j d_{0j} \Gamma_j^{(1)}(t') \phi_j \\ &= \sum_{j,f} I_{2,j,f}(t) \phi_f \end{aligned} \quad (\text{A11})$$

with the transitions amplitudes

$$I_{2,j,f}(t) = -i \int_{-\infty}^t dt' \sum_{j,f} \langle \phi_j | H_p | \phi_f \rangle d_{0j} \Gamma_j^{(1)}(t'). \quad (\text{A12})$$

The summation is over all possible intermediate j and final f states, to which the transitions are allowed. Therefore, the time evolution of the second order wave function can be expressed as

$$\Psi_2(t) = \sum_{j,f} d_{0j} d_{jf} \Gamma_{j,f}^{(2)}(t) \phi_f. \quad (\text{A13})$$

The function $\Gamma_{j,f}^{(2)}(t)$ is obtained by the substitution of H_p and $\Gamma_j^{(1)}(t)$ into Eq. (A12):

$$\begin{aligned} \Gamma_{j,f}^{(2)}(t) &= \frac{2(\epsilon_f - \epsilon_j)(\epsilon_j - \epsilon_0)}{\sqrt{\pi}} \left(\frac{\mathcal{N} T}{2\pi c} \right)^2 \\ &\times \int_{-\infty}^{t/T} ds' \left[e^{i(\epsilon_f - \epsilon_j)Ts'} \cos(\omega_0 Ts') e^{-s'^2} \right. \\ &\times \left[e^{-\frac{[T(\omega_0 j + \omega_0)]^2}{4}} \text{erfc}\left(\frac{i}{2} T(\omega_0 j + \omega_0) - s'\right) \right. \\ &\left. \left. + e^{-\frac{[T(\omega_0 j - \omega_0)]^2}{4}} \text{erfc}\left(\frac{i}{2} T(\omega_0 j - \omega_0) - s'\right) \right] \right]. \end{aligned} \quad (\text{A14})$$

We neglected the term $\mathbf{A}^2/2c^2$ in the Hamiltonian function $H_p(t)$ for the following reason. If we substitute this part to the integral (A4), we obtain

$$\begin{aligned} &-i \int_{-\infty}^t dt' e^{i(\epsilon_f - \epsilon_0)t'} \langle \phi_f | \frac{1}{2c^2} \mathbf{A}^2 | \Psi_0 \rangle \\ &= -\frac{i}{4c^2} \int_{-\infty}^t dt' (\mathcal{N} f)^2 e^{i(\epsilon_f - \epsilon_0)t'} \langle \phi_f | 1 + \cos(2\omega_0 t) | \Psi_0 \rangle. \end{aligned} \quad (\text{A15})$$

The transition matrix element is diagonal in the electronic states and does not give rise to any transitions.

APPENDIX B: THE CALCULATION OF THE SECOND ORDER WAVE FUNCTION IN THE HYDROGEN ATOMLIKE SYSTEM

In order to derive the dipole matrix elements, one has first to recall the wave functions of levels in a hydrogen atom.³⁷ The wave functions of the 1s state are

$$\Psi_{jj_z}^{1s} = R_{1s} \psi_{jj_z}, \quad (\text{B1})$$

where $j = 1/2$ is the total orbital momentum, $j_z = \pm 1/2$ is the projection of the momentum on the z direction, $R_{1s} = 2e^{-r}$ is the radial part, and ψ_{jj_z} is the spherical part.

$$\psi_{1/2, \pm 1/2} = Y_{00} \chi_{\pm}, \quad (\text{B2})$$

where $Y_{00} = Y_{l=0, m_l=0} = \sqrt{\frac{1}{4\pi}}$ is the spherical harmonic function, and χ_{\pm} are the spinor functions: $\chi_+ = \begin{pmatrix} 1 \\ 0 \end{pmatrix}$, $\chi_- = \begin{pmatrix} 0 \\ 1 \end{pmatrix}$.

Similarly, the wave functions of the 2p state are

$$\Psi_{jj_z}^{2p} = R_{2p} \psi_{jj_z} \quad (\text{B3})$$

with the radial function $R_{2p} = \frac{1}{2\sqrt{6}} r e^{-r/2}$ and the spherical functions

$$\begin{aligned} \psi_{3/2, 3/2} &= Y_{11} \chi_+, \quad \psi_{3/2, 1/2} = \sqrt{\frac{2}{3}} Y_{10} \chi_+ + \sqrt{\frac{1}{3}} Y_{11} \chi_-, \\ \psi_{3/2, -1/2} &= \sqrt{\frac{2}{3}} Y_{10} \chi_- + \sqrt{\frac{1}{3}} Y_{1-1} \chi_+, \quad \psi_{3/2, -3/2} = Y_{1-1} \chi_-, \\ \psi_{1/2, 1/2} &= \sqrt{\frac{1}{3}} Y_{10} \chi_+ - \sqrt{\frac{2}{3}} Y_{11} \chi_-, \\ \psi_{1/2, -1/2} &= \sqrt{\frac{1}{3}} Y_{10} \chi_- - \sqrt{\frac{2}{3}} Y_{1-1} \chi_+, \end{aligned} \quad (\text{B4})$$

with the spherical harmonics

$$\begin{aligned} Y_{10} &= \sqrt{\frac{3}{4\pi}} \frac{z}{r}, \quad Y_{11} = \sqrt{\frac{3}{8\pi}} \frac{y - ix}{r}, \\ Y_{1-1} &= \sqrt{\frac{3}{8\pi}} \frac{y + ix}{r}. \end{aligned} \quad (\text{B5})$$

The dipole matrix elements of the transitions from the $1s$ to $2p$ state are $\int d^3r \Psi_{j'j_z'}^{2p*} \mathbf{z} \mathcal{D} \Psi_{jj_z}^{1s}$. We assumed that the spin is initially in the x direction. It means that the ground state wave function is

$$\Psi_0 = Y_{00} R_{1s} \frac{1}{\sqrt{2}} (\chi_+ + \chi_-). \quad (\text{B6})$$

Therefore, the dipole matrix elements of transitions from the ground state to the excited states in our system are

$$\begin{aligned} &\int d^3r \Psi_{jj_z}^{2p*} \frac{x + iy}{\sqrt{2}} \Psi_0 \\ &= \int d^3r R_{2p} \Psi_{jj_z}^* \frac{x + iy}{\sqrt{2}} Y_{00} R_{1s} \frac{1}{\sqrt{2}} (\chi_+ + \chi_-). \end{aligned} \quad (\text{B7})$$

The spinors, entering the integrals, obey the relations $\chi_{\pm}^* \chi_{\mp} = 0$, $\chi_{\pm}^* \chi_{\pm} = 1$. Examining the wave functions of the $2p$ state [Eq. (B4)], one can see that there are three types of integrals entering (B7):

$$\begin{aligned} &\int d^3r Y_{11}^* R_{2p} \frac{x + iy}{\sqrt{2}} Y_{00} R_{1s} \\ &= \int d^3r \frac{1}{\sqrt{2}} \frac{1}{2\sqrt{6}} r e^{-r/2} \sqrt{\frac{3}{8\pi}} \frac{y + ix}{r} (x + iy) \sqrt{\frac{1}{4\pi}} 2e^{-r} \\ &= -i \frac{2^{15/2}}{3^5} d_0 \end{aligned} \quad (\text{B8})$$

$$\int d^3r Y_{10}^* R_{2p} \frac{x + iy}{\sqrt{2}} Y_{00} R_{1s} \propto \int d^3r z (x + iy) = 0 \quad (\text{B9})$$

$$\begin{aligned} &\int d^3r Y_{1-1}^* R_{2p} \frac{x + iy}{\sqrt{2}} Y_{00} R_{1s} \propto \int d^3r (y - ix)(x + iy) \\ &= -i \int d^3r (x^2 - y^2) = 0. \end{aligned} \quad (\text{B10})$$

Therefore, there are only three nonzero dipole matrix elements of the transitions from the ground state to the excited states induced by circularly polarized laser light:

$$\begin{aligned} d_{01} &= \int d^3r \Psi_{3/2,3/2}^{2p*} \frac{x + iy}{\sqrt{2}} \Psi_0 \\ &= \frac{1}{\sqrt{2}} \int d^3r \Psi_{3/2,3/2}^{2p*} \frac{x + iy}{\sqrt{2}} \Psi_{1/2,1/2}^{1s} = \frac{1}{\sqrt{2}} d_0; \end{aligned} \quad (\text{B11})$$

another to $\{2p, j = 3/2, j_z = 1/2\}$:

$$\begin{aligned} d_{02} &= \int d^3r \Psi_{3/2,1/2}^{2p*} \frac{x + iy}{\sqrt{2}} \Psi_0 \\ &= \frac{1}{\sqrt{2}} \int d^3r \Psi_{3/2,1/2}^{2p*} \frac{x + iy}{\sqrt{2}} \Psi_{1/2,-1/2}^{1s} = \frac{1}{\sqrt{2}} \sqrt{\frac{1}{3}} d_0; \end{aligned} \quad (\text{B12})$$

and one to $\{2p, j = 1/2, j_z = 1/2\}$:

$$\begin{aligned} d_{03} &= \int d^3r \Psi_{1/2,1/2}^{2p*} \frac{x + iy}{\sqrt{2}} \Psi_0 \\ &= \frac{1}{\sqrt{2}} \int d^3r \Psi_{1/2,1/2}^{2p*} \frac{x + iy}{\sqrt{2}} \Psi_{1/2,-1/2}^{1s} = -\frac{1}{\sqrt{2}} \sqrt{\frac{2}{3}} d_0. \end{aligned} \quad (\text{B13})$$

Likewise, there are three allowed transitions from the excited states back to the $1s$ state:

(1) to the spin-up state from the $\{2p, j = 3/2, j_z = 3/2\}$ state with the dipole matrix element $d_{10} = d_0^*$,

(2) to the spin-down state from $\{2p, j = 3/2, j_z = 1/2\}$ with $d_{20} = \sqrt{1/3} d_0^*$, and

(3) to the spin-down state from $\{2p, j = 1/2, j_z = 1/2\}$ with $d_{30} = -\sqrt{2/3} d_0^*$.

The time-dependent parts $\Gamma^{(2)}(t)$, which enter Eq. (8), depend on the energies of initial, intermediate, and final states. Since we assumed that the SOC in our system is considerable and the $2p$ state is split, two functions $\Gamma^{(2)}(t)$ can be distinguished: the one for the transitions to the excited states with $j = 3/2$, designated as $\Gamma_{3/2}^{(2)}(t)$, and for $j = 1/2$, designated as $\Gamma_{1/2}^{(2)}(t)$. Applying Eq. (8) to our system, we obtain the second order wave function, which describes the stimulated Raman scattering process:

$$\begin{aligned} \Psi_2(t) &= d_{01} d_{10} \Gamma_{3/2}^{(2)}(t) \Psi_{1/2}^{1s} + d_{02} d_{20} \Gamma_{3/2}^{(2)}(t) \Psi_{-1/2}^{1s} \\ &\quad + d_{03} d_{30} \Gamma_{1/2}^{(2)}(t) \Psi_{-1/2}^{1s} \\ &= \frac{1}{\sqrt{2}} \left(|d_0|^2 \Gamma_{3/2}^{(2)}(t) \chi_+ + \frac{1}{3} |d_0|^2 \Gamma_{3/2}^{(2)}(t) \chi_- \right. \\ &\quad \left. + \frac{2}{3} |d_0|^2 \Gamma_{1/2}^{(2)}(t) \chi_- \right) Y_{00} R_{1s} \\ &= \frac{|d_0|^2}{\sqrt{2}} \left(\frac{\Gamma_{3/2}^{(2)}(t)}{\frac{1}{3} \Gamma_{3/2}^{(2)}(t) + \frac{2}{3} \Gamma_{1/2}^{(2)}(t)} \right) Y_{00} R_{1s}. \end{aligned} \quad (\text{B14})$$

APPENDIX C: THE EFFECT OF LINEAR POLARIZED LIGHT

If the light was linear, there would be no spin rotation in the system. For example, for linear light in the x direction, the integrals entering (B7) are

$$\begin{aligned} &\int d^3r Y_{11}^* R_{2p} x Y_{00} R_{1s} \\ &= \int d^3r \frac{1}{\sqrt{6}} \sqrt{\frac{1}{4\pi}} r e^{-3r/2} \sqrt{\frac{3}{8\pi}} \frac{y + ix}{r} x = i d_x, \\ &\int d^3r Y_{10}^* R_{2p} x Y_{00} R_{1s} \\ &\propto \int d^3r z x = 0, \\ &\int d^3r Y_{1-1}^* R_{2p} x Y_{00} R_{1s} \\ &= \int d^3r \frac{1}{\sqrt{6}} \sqrt{\frac{1}{4\pi}} r e^{-3r/2} \sqrt{\frac{3}{8\pi}} \frac{y - ix}{r} x = -i d_x. \end{aligned} \quad (\text{C1})$$

And the second order wave function in the case of linear light would be

$$\begin{aligned}\Psi_2^{ln}(t) &= \frac{|d_x|^2}{\sqrt{2}} \left(\Gamma_{3/2}^{(2)}(t) + \frac{1}{3} \Gamma_{3/2}^{(2)}(t) - \frac{2}{3} \Gamma_{1/2}^{(2)}(t) \right) Y_{00} R_{1s} \\ &= |d_x|^2 \left(\frac{4}{3} \Gamma_{3/2}^{(2)}(t) - \frac{2}{3} \Gamma_{1/2}^{(2)}(t) \right) Y_{00} R_{1s} \left(\frac{1}{\sqrt{2}} \right).\end{aligned}\quad (C2)$$

The spinor of the function would always correspond to the alignment of the spin in the x direction, and no rotation could be observed. It can be easily reproduced for linear light in any direction.

APPENDIX D: THE ACTION OF POLARIZED LIGHT ON ANTICOLLINEAR SYSTEMS

We show in this Appendix that if the alignments of spin systems were initially anticollinear, then the systems are rotated by different angles due to the action of circularly polarized light. We check it with two equal hydrogen atomlike models. The spin of the first one is aligned initially in the x direction, and the spin of the second one is in the $-x$ direction. The wave function, describing the $1s$ state of the first system during and after the action of the pulse, is $\Psi_{1s}^{+x}(t) = \Psi_0^{+x} + \Psi_2^{+x}(t)$, which is according to Eqs. (B6) and (B14)

$$\Psi_{1s}^{+x}(t) = \left(\frac{1}{\sqrt{2}} + \frac{|d_0|^2 \Gamma_{3/2}^{(2)}(t)}{\sqrt{2}} \right) Y_{00} R_{1s}. \quad (D1)$$

The initial wave function Ψ_0^{-x} of the system with spin aligned in the $-x$ direction is

$$\Psi_0^{-x} = \begin{pmatrix} \Psi_{1/2}^{1s} \\ -\Psi_{-1/2}^{1s} \end{pmatrix} = \begin{pmatrix} \frac{1}{\sqrt{2}} \\ \frac{1}{\sqrt{2}} \end{pmatrix} Y_{00} R_{1s}. \quad (D2)$$

The procedure to obtain the second order wave function $\Psi_2^{-x}(t)$ described in Appendix B would be equal for this system except that the function $\Psi_{-1/2}^{1s}$ in Eq. (B14) enters with the negative sign. Therefore, the wave function $\Psi_{1s}^{-x}(t) = \Psi_0^{-x} + \Psi_2^{-x}(t)$ of the second system is

$$\Psi_{1s}^{-x}(t) = \begin{pmatrix} \frac{1}{\sqrt{2}} + \frac{|d_0|^2 \Gamma_{3/2}^{(2)}(t)}{\sqrt{2}} \\ -\frac{1}{\sqrt{2}} - \frac{|d_0|^2 \left(\frac{1}{3} \Gamma_{3/2}^{(2)}(t) + \frac{2}{3} \Gamma_{1/2}^{(2)}(t) \right)}{\sqrt{2}} \end{pmatrix} Y_{00} R_{1s}. \quad (D3)$$

We calculate the expectation value of the orientation of both systems due to the action of light ($e_x^\pm, e_y^\pm, e_z^\pm$) with the help of Pauli matrices σ_α (α stands for x, y, z) as follows:

$$e_\alpha^\pm = \frac{\langle \Psi_{1s}^{\pm x}(t) | \sigma_\alpha | \Psi_{1s}^{\pm x}(t) \rangle}{|\Psi_{1s}^{\pm x}(t)|^2}. \quad (D4)$$

Substituting $\psi_{1s}^\uparrow(t)$ for $(1/\sqrt{2})[1 + |d_0|^2 \Gamma_{3/2}^{(2)}(t)]$ and $\psi_{1s}^\downarrow(t)$ for $(1/\sqrt{2})[1 + |d_0|^2 (\frac{1}{3} \Gamma_{3/2}^{(2)}(t) + \frac{2}{3} \Gamma_{1/2}^{(2)}(t))]$, the components of the vectors \mathbf{e}^+ and \mathbf{e}^- are

$$\begin{aligned}e_x^+ &= -e_x^- = \frac{1}{2} \frac{\psi_{1s}^\uparrow(t) \psi_{1s}^{\downarrow*}(t) + \text{c.c.}}{|\psi_{1s}^\uparrow(t)|^2 + |\psi_{1s}^\downarrow(t)|^2}, \\ e_y^+ &= -e_y^- = \frac{1}{2} \frac{i[\psi_{1s}^\uparrow(t) \psi_{1s}^{\downarrow*}(t) - \text{c.c.}]}{|\psi_{1s}^\uparrow(t)|^2 + |\psi_{1s}^\downarrow(t)|^2}, \\ e_z^+ &= e_z^- = \frac{1}{2} \frac{|\psi_{1s}^\uparrow(t)|^2 - |\psi_{1s}^\downarrow(t)|^2}{|\psi_{1s}^\uparrow(t)|^2 + |\psi_{1s}^\downarrow(t)|^2}.\end{aligned}\quad (D5)$$

Thus, the projections of the two spins on the xy plane are opposite, and the projections on the z axis are equal. This example shows that although two equal antiparallel spin systems were collinear, the action of circularly polarized light led to the deviation from their initial state by different angles.

¹Alexey V. Kimel, Andrei Kirilyuk, and Theo Rasing, *Laser Photon. Rev.* **1**, 275 (2007).

²Andrei Kirilyuk, Alexey V. Kimel, and Theo Rasing, *Rev. Mod. Phys.* **82**, 2731 (2010).

³L. P. Pitaevskii, *Sov. Phys. JETP* **12**, 1008 (1961).

⁴P. S. Pershan, J. P. van der Ziel, and L. D. Malmstrom, *Phys. Rev.* **143**, 574 (1966).

⁵Y. R. Shen, *The Principles of Nonlinear Optics* (Wiley, New York, 1984).

⁶A. V. Kimel, A. Kirilyuk, A. Tsvetkov, R. V. Pisarev, and Th. Rasing, *Nature (London)* **429**, 850 (2004).

⁷A. V. Kimel, A. Kirilyuk, P. A. Usachev, R. V. Pisarev, A. M. Balbashov, and Th. Rasing, *Nature (London)* **435**, 655 (2005).

⁸A. V. Kimel, C. D. Stanciu, P. A. Usachev, R. V. Pisarev, V. N. Gridnev, A. Kirilyuk, and Th. Rasing, *Phys. Rev. B* **74**, 060403R (2006).

⁹Fredrik Hansteen, Alexey Kimel, Andrei Kirilyuk, and Theo Rasing, *Phys. Rev. B* **73**, 014421 (2006).

¹⁰C. D. Stanciu, F. Hansteen, A. V. Kimel, A. Tsukamoto, A. Itoh, A. Kirilyuk, and Th. Rasing, *Phys. Rev. Lett.* **98**, 207401 (2007).

¹¹A. M. Kalashnikova, A. V. Kimel, R. V. Pisarev, V. N. Gridnev, P. A. Usachev, A. Kirilyuk, and Th. Rasing, *Phys. Rev. B* **78**, 104301 (2008).

¹²T. Satoh, Sung-Jin Cho, R. Iida, T. Shimura, K. Kuroda, H. Ueda, Y. Ueda, B. A. Ivanov, F. Nori, and M. Fiebig, *Phys. Rev. Lett.* **105**, 077402 (2010).

¹³A. H. M. Reid, A. V. Kimel, A. Kirilyuk, J. F. Gregg, and Th. Rasing, *Phys. Rev. B* **81**, 104404 (2010).

¹⁴R. Iida, T. Satoh, T. Shimura, K. Kuroda, B. A. Ivanov, Y. Tokunaga, and Y. Tokura, *Phys. Rev. B* **84**, 064402 (2011).

¹⁵A. V. Kimel, B. A. Ivanov, R. V. Pisarev, P. A. Usachev, A. Kirilyuk, and Th. Rasing, *Nat. Phys.* **5**, 727 (2009).

¹⁶J.-Y. Bigot, M. Vomer, L. H. F. Andrade, and E. Beaupaire, *Chem. Phys.* **318**, 137 (2005).

¹⁷Jean-Yves Bigot, Mircea Vomer, and Eric Beaupaire, *Nat. Phys.* **5**, 515 (2009).

- ¹⁸C. Boeglin, E. Beaurepaire, V. Halté, V. Lopez-Flores, C. Stamm, N. Pontius, H. A. Dürr, and J.-Y. Bigot, *Nature (London)* **465**, 458 (2010).
- ¹⁹R. Gómez-Abal and W. Hübner, *J. Phys. Condens. Matter* **15**, 709 (2003).
- ²⁰V. N. Gridnev, *Phys. Rev. B* **77**, 094426 (2008).
- ²¹G. Lefkidis, G. P. Zhang, and W. Hübner, *Phys. Rev. Lett.* **103**, 217401 (2009).
- ²²M. I. Kurkin, N. B. Bakulina, and R. V. Pisarev, *Phys. Rev. B* **78**, 134430 (2008).
- ²³S. R. Woodford, A. Bringer, and S. Blügel, *J. Appl. Phys.* **101**, 053912 (2007).
- ²⁴S. R. Woodford, *Phys. Rev. B* **79**, 212412 (2009).
- ²⁵A. Yu. Galkin and B. A. Ivanov, *JETP Lett.* **88**, 249 (2008).
- ²⁶C. A. Perroni and A. Liebsch, *Phys. Rev. B* **74**, 134430 (2006).
- ²⁷Riccardo Hertel, *J. Magn. Magn. Mater.* **303**, L1 (2006).
- ²⁸D. Popova, A. Bringer, and S. Blügel, *Phys. Rev. B* **84**, 214421 (2011).
- ²⁹J. P. van der Ziel, P. S. Pershan, and L. D. Malmstrom, *Phys. Rev. Lett.* **15**, 190 (1965).
- ³⁰Natsuki Kanda, Takuya Higuchi¹, Hirokatsu Shimizu, Kuniaki Konishi, Kosuke Yoshioka, and Makoto Kuwata-Gonokami, *Nat. Commun.* **2**, 362 (2011).
- ³¹Rodney Loudon, *The Quantum Theory of Light* (Clarendon Press, Oxford, 1973).
- ³²*Handbook of Mathematical Functions*, edited by M. Abramowitz and I. A. Stegun (Dover Publications, Mineola, NY, 1972).
- ³³J. M. Bao, A. V. Bragas, J. K. Furdyna, and R. Merlin, *Phys. Rev. B* **71**, 045314 (2005).
- ³⁴M. V. Gurudev Dutt, J. Cheng, B. Li, X. Xu, X. Li, P. R. Berman, D. G. Steel, A. S. Bracker, D. Gammon, S. E. Economou, R. B. Liu, and L. J. Sham, *Phys. Rev. Lett.* **94**, 227403 (2005).
- ³⁵Yanwen Wu, Erik D. Kim, Xiaodong Xu, Jun Cheng, D. G. Steel, A. S. Bracker, D. Gammon, Sophia E. Economou, and L. J. Sham, *Phys. Rev. Lett.* **99**, 097402 (2007).
- ³⁶Jun Cheng, Wang Yao, Xiaodong Xu, D. G. Steel, A. S. Bracker, D. Gammon, and L. J. Sham, *Phys. Rev. B* **77**, 115315 (2008).
- ³⁷L. D. Landau and E. M. Lifshitz, *Quantum Mechanics: Non-Relativistic Theory*, 3rd ed., Vol 3 (Pergamon Press, Oxford, 1977).
- ³⁸Yu. Ralchenko, A. E. Kramida, and J. Reader, and NIST ASD Team, *NIST Atomic Spectra Database*, ver. 4.0.1 (National Institute of Standards and Technology, Gaithersburg, MD, 2010), [<http://physics.nist.gov/asd>].
- ³⁹I. S. Gradshteyn and I. M. Ryzhik, *Tables of Integrals, Series and Products* (Academic Press, New York, 1965).